

MAPPING THE RADIO EMISSION FROM MASSIVE YOUNG STELLAR OBJECTS

MELVIN G. HOARE AND JANET E. DREW

Department of Physics, Astrophysics, University of Oxford, Keble Road, Oxford, OX1 3RH, U.K.

AND

TOM B. MUXLOW AND RICHARD J. DAVIS¹

Nuffield Radio Astronomy Laboratory, Jodrell Bank, Lower Withington, Cheshire, SK11 9DL, U.K.

Received 1993 October 25; accepted 1993 November 12

ABSTRACT

We present the first maps of the radio emission from hitherto spatially unresolved massive young stellar objects. Observations of three targets were made with the recently upgraded MERLIN array at 5 GHz with a nominal resolution of 0".05. Our map of the exciting source of the bipolar H II region S106 reveals a source of 0".224 × 0".060 elongated perpendicular to the H II region. This could be due to interaction of the stellar wind with a remnant disk, enhancement of the wind in the equatorial plane due to rapid rotation of the young star, or a disk-fed radiation-driven wind. By comparison, the emission from LkH α 101 is symmetric, although rather clumpy. No emission was detected from BN to a level of 0.3 mJy beam⁻¹.

Subject headings: radio continuum: stars — stars: early-type — stars: individual (S106IR) — stars: individual (LkH α 101) — stars: mass loss

1. INTRODUCTION

The mass loss that invariably occurs during the early stages of a star's life is an important aspect of the overall process of star formation. In high-mass young stellar objects (YSOs) mass loss via an ionized wind is implied by broad near-IR line emission (e.g., Persson et al. 1984) and radio continuum emission with a spectral index close to that expected for a constant velocity outflow (e.g., Simon et al. 1981). This is often accompanied by bipolar molecular outflow on a much larger scale (e.g., Lada 1985). These objects (often called BN objects after the prototype in Orion) are deeply embedded in their natal molecular clouds and therefore totally obscured in the optical while being very luminous in the IR.

The mechanism responsible for driving the ionized winds in the early stages of a massive star's life is not known. Whenever hot luminous stars are concerned it is natural to consider radiation pressure as a strong candidate, although luminous YSO winds appear to be much slower and denser than the reasonably well-understood radiation-driven winds seen in field main-sequence stars. If the star has not reached the main sequence then it may drive a wind similar to the low-gravity OB supergiants and hypergiants (see also Hamann & Persson 1989). If an active accretion disk is present then this could also be responsible for driving the wind either via radiation pressure or a magneto-hydrodynamic mechanism (e.g., Pudritz & Norman 1986). The effect of a disk is often invoked to explain the bipolar morphologies of the associated large-scale molecular outflows. This symmetry apparently can persist to later stages when the star has ionized a substantial region of the surrounding ISM to form a bipolar H II region such as S106 (Solf & Carsenty 1982).

Clues to the driving mechanism, and therefore to how the mass loss fits into the wider star formation picture, could be gained from defining the morphology of the ionized wind.

These winds are predicted to recombine within a few tens of AU from the star (Simon et al. 1983; Höflich & Wehrse 1987) which corresponds to less than 0".1 at a typical distance of 1 kpc. Therefore, at present, radio interferometry offers the only prospect of directly resolving the spatial structure of these winds. Observations with the VLA have succeeded only in partially resolving the emission from two of the brightest objects, BN itself (Churchwell et al. 1987; Felli et al. 1993) and LkH α 101 (Becker & White 1988), another more evolved source which excites a large H II region. In this *Letter* we report observations with the recently upgraded MERLIN array which now has sufficient resolution and sensitivity to map these sources for the first time. We observed the three brightest massive YSOs at 5 GHz, the first frequency available with MERLIN Phase 2. These were BN, LkH α 101, and S106IR, the exciting source of the bipolar H II region mentioned above.

2. OBSERVATIONS

Observations were made with the full MERLIN array with a bandwidth of 30 MHz at a frequency of 5 GHz for a full track on each object. The system employs cooled HEMT receivers with a system temperature of around 30 K. The maximum baseline length was 218 km giving a resolution of 50 mas. The observations were amplitude calibrated against OQ 208 whose flux density was measured to be 2.52 Jy by calibration against short spacing observations on 3C 286 whose flux density was assumed to be 7.02 Jy.

The observations were made in phase referencing mode in which 7 minute observations on each target were interspersed with 1 minute observations of a nearby VLBI point-source calibrator with astrometric (~ 2 mas) accuracy. The phase reference sources used were 2023 + 335 for S106IR, 0440 + 345 for LkH α 101, and 0539 – 057 for BN. The angular separations of the target and the reference sources are $\sim 2^\circ$. Initial data reduction was carried out using the local OLAF package, and the data were mapped using standard phase-referencing techniques in the NRAO Astronomical Image Processing System (AIPS). Complex telescope gain solutions were derived by

¹ On leave of absence at the National Radio Astronomy Observatory, P.O. Box O, Socorro, New Mexico 87801, which is run by Associated Universities, Inc., under the National Science Foundation.

applying self-calibration to the phase reference source only, and these solutions were applied to the target source. The data were then mapped and CLEANed (Clark 1980) to produce the final images.

3. RESULTS

3.1. S106IR

In the map made with the fully-synthesized, uniformly weighted beam no source is visible above the rms noise level of 0.12 mJy. The noise level is significantly higher than the 0.06 mJy rms level attainable with MERLIN at 5 GHz because of the confusion caused by the extended emission from the surrounding H II region. However, on applying natural weighting and a $3M\lambda$ taper a significant detection of the central source is achieved as shown in Figure 1. The peak flux is about 10 times the rms noise level in the map and corresponds to a brightness temperature of about 18,000 K. The total integrated flux in the map in Figure 1 is 8.9 ± 0.9 mJy which is considerably larger than the 5.4 ± 0.2 mJy measured with the VLA in a $0''.5$ beam by Bally, Snell, & Predmore (1983). Those authors cautioned that they may have underestimated the flux due to the proximity of a negative side lobe in their map. Note that we also have a significant negative sidelobe in our map to the NE of the source that may slightly affect our flux determination.

The source is clearly resolved into an elongated structure by the $0''.1$ beam. Although the negative sidelobe may be affecting the morphology of the source on the NE side, no such problems occur on the SW side. A two-dimensional Gaussian fit using the AIPS routine IMFIT gives the observed source dimensions as $0''.246 \times 0''.116$ and a deconvolved size of $0''.224 \times 0''.060$ at a P.A. = $119^\circ \pm 5^\circ$. At a distance of 600 pc (Staude et al. 1982) this corresponds to 134×36 AU. This result is consistent with the upper limit of $0''.15$ on the size of S106IR at 23 GHz from VLA observations by Felli et al. (1985). The size of the emitting region for a stellar wind scales as $v^{-0.6}$ (Wright & Barlow 1975) so at 23 GHz the major axis of the emission seen in Figure 1 would be $0''.09$.

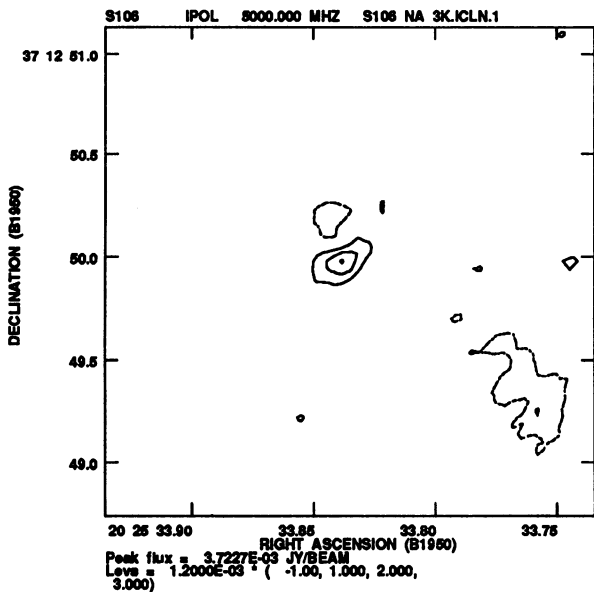


FIG. 1.—5 GHz map of S106IR made with a $0''.105 \times 0''.097$ beam at P.A. = -32° .

It is interesting to relate the orientation of the radio emission from S106IR to that of the bipolar H II region it excites. From the radio maps of Bally et al. (1983) we estimate that the position angle (P.A.) of the bipolar lobes is $29^\circ \pm 2^\circ$, and so the equatorial plane lies at $119^\circ \pm 2^\circ$. Hence the radio emission is extended along the equatorial plane.

3.2. LkH α 101

With a 5 GHz flux of 32 ± 2 mJy as measured by the VLA (Becker & White 1988) LkH α 101 was easily detected by MERLIN revealing a source about $0''.4$ in diameter. However, it was somewhat overresolved at the full resolution of $0''.053 \times 0''.047$ with the emission breaking up into several peaks. A slightly smoothed map is shown in Figure 2 where the dimensions of the source are $0''.342 \times 0''.284$ at P.A. = $97^\circ \pm 10^\circ$. This is consistent with the effective 5 GHz diameter of $0''.33$ deduced by Becker & White (1988) from fitting the VLA visibility function and corresponds to a linear diameter of 250 AU at 800 pc (Herbig 1971). The peak brightness temperature in our map is 12,000 K while the total flux in our map is 15 ± 1 mJy, that is, MERLIN has resolved out some of the more extended emission associated with this source.

3.3. BN

We did not detect BN in either fully synthesized or tapered maps. The 3σ upper limit is 0.30 mJy in a $0''.050$ beam which corresponds to a brightness temperature of 6,000 K. The only reported detections of BN at 5 GHz are 2.2 ± 0.8 mJy by Felli et al. (1993) and 1.1 mJy by Garay (1987) which would have been detected by MERLIN if the source has a diameter of $\approx 0''.11$. Partially resolved VLA observations indicate sizes of $\sim 0''.1$ at 15 GHz (Churchwell et al. 1987) and 22 GHz (Menten & Reid 1990). A stellar wind origin would mean that BN was $\geq 0''.2$ at 5 GHz, enough to take the surface brightness below the quoted MERLIN upper limits.

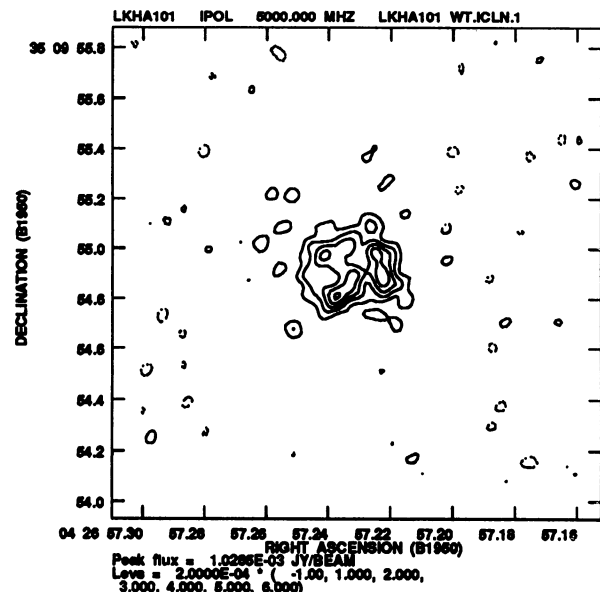


FIG. 2.—5 GHz map of LkH α 101 made with a $0''.065$ circular beam

4. DISCUSSION

4.1. S106IR

Presented with the map in Figure 1, one may be tempted to say that we are simply seeing emission from an ionized disk seen nearly edge-on rather than a stellar wind. Solf & Carsenty (1982) used the kinematics of the bipolar nebula to deduce that the inclination angle of the system in the plane of the sky is about 75° . The aspect ratio we observe of $4.2 \pm 1.2:1$ is consistent with the expected foreshortening of a thin disk of $1/\cos 75^\circ = 3.9$. However, the broad near-IR H I emission lines and the recently discovered blueshifted absorption seen in the He I 2.058 μm line (Drew, Bunn, & Hoare 1993) point overwhelmingly to the presence of strong mass loss in this system. Wind models that explain the near-IR line fluxes also match the radio fluxes (e.g., Höflich & Wehrse 1987), and the previously published radio spectral index of 0.75 ± 0.07 (Bally et al. 1983) is close to that expected for a constant velocity outflow (Wright & Barlow 1975). Schmid-Burgk (1982) showed that the spectral index is not very sensitive to the wind geometry.

4.1.1. Equatorial Wind

One possible explanation for the radio morphology of S106IR is that its wind is predominately equatorial. This has been put forward before in order to explain how the exciting source can simultaneously ionize the H II region in the polar direction and not the lane between the lobes where there is a gap in the radio emission (e.g., Felli et al. 1984). As for the physical mechanism one should consider whether rotation of the star is somehow involved, assuming that the rotation axis of the star is aligned with that of the H II region.

Recently, Bjorkman & Cassinelli (1993) have carried out an analytic two-dimensional investigation of the effect of rotation on radiatively driven winds from main-sequence OB stars. They showed that even for modest rotation rates there is a significant increase in density in the equatorial plane while at higher rotation rates a "wind-compressed-disk" forms. Numerical simulations by Owocki, Cranmer, & Blondin (1993) support this basic concept but predict a somewhat lower density contrast between the equator and the pole. For instance, their standard model for a B2 V star with $\Omega = v_{\text{rot}}/v_{\text{crit}} = 0.4$ predicts a equator/pole density ratio of 2.5. Since the radio emission scales as n_e^2 and we are viewing S106IR nearly edge-on this magnitude of density contrast is near the minimum required to explain the observed 4:1 aspect ratio.

There is as yet no definite measurement of the rotation speed of S106IR. The possible detection of a photospheric component to the He I 2.058 μm line by Drew et al. (1993) would limit v_{rot} to about 90 km s^{-1} . A main-sequence star at the luminosity of S106IR ($4 \times 10^4 L_\odot$, Mozurkewich, Schwartz, & Smith 1986) (B0 V) would have a critical velocity of $\sim 600 \text{ km s}^{-1}$ which would imply $\Omega \lesssim 0.15$. However, if the wind is driven by radiation pressure as required in this picture, then the high mass-loss rate and low terminal velocity for the wind means that the star must have a much lower surface gravity and hence critical velocity than a main-sequence star. This scenario needs a much better determination of the stellar parameters (T_{eff} , $\log g$, R , $v \sin i$) to test it.

4.1.2. Effect of a Disk

It is generally thought that when stars form they accrete mass and lose angular momentum via a disk. If such a disk is still present in the system, it could be responsible for the radio morphology. Hydromagnetic disk winds have been put

forward to explain the bipolar molecular flows in YSOs, although these may impart a rather higher rotational component in the near-IR emission lines than is seen.

Another possibility is that even if the wind originates from the star and is initially isotropic it is somehow enhanced in the equatorial plane by the presence of a remnant disk of material. Evidence for a circumstellar disk in S106IR has recently come from high spectral resolution observations of strong emission lines in the first overtone bands of CO at 2.3 μm by Chandler et al. (1993). Persson, McGregor, & Campbell (1988) also claim that the double-peaked Ca II triplet line profiles are indicative of formation in a disk, although the blueshifted central absorption could also be interpreted as self-absorption formed in an outflow.

If there is a circumstellar disk of material how could this enhance the stellar wind? One way is for an initially isotropic stellar wind to interact dynamically with the remnant disk, picking up mass as it sweeps over the surface layers. However, calculations by J. M. Porter (1993, private communication) have shown that in order for ram-pressure stripping to result in significant mass-loading of the wind, the mass-loss rate of the wind must be very high ($\approx 10^{-5} M_\odot \text{ yr}^{-1}$). In which case we are still left with the problem of how to explain the high mass-loss rate from the star itself. A similar objection can be raised to the disk photo-evaporation mechanism as discussed by Hollenbach, Johnstone, & Shu (1993). In this scenario the heating by diffuse Lyman continuum photons causes the outer ($r \gtrsim 100 \text{ AU}$), low surface gravity regions of the disk to evaporate steadily from the disk surface at 10–50 km s^{-1} . However, this cannot explain the high-velocity wings on the H I lines, and so again we still need another mechanism for the strong stellar wind.

A simpler picture, perhaps able to explain all the observed phenomena, is one in which radiation pressure from the star acts directly on the loosely bound material in the atmosphere of the inner disk ($\lesssim 10 R_*$ or 1 AU). The same line-driving mechanism known to operate in normal OB stars would force material away laterally and could easily reach velocities of several hundred km s^{-1} (see discussion in Drew et al. 1993).

4.2. Comparison with LkH α 101

Why does the radio morphology of LkH α 101 appear reasonably symmetric compared to that of S106IR? One possibility is that the wind from LkH α 101 is also equatorial but the star is orientated such that we see it nearly face-on. Unfortunately there are few clues as to the inclination of LkH α 101; for example, it does not drive an organized bipolar molecular outflow (Barsony et al. 1990).

Alternatively LkH α 101 may be in a different evolutionary phase to S106IR. There are significant differences in the near-IR lines inasmuch as the H I emission lines in LkH α 101 are much stronger and narrower than those in S106IR and the high-velocity wings much less prominent (Simon & Cassar 1984; Drew et al. 1993). Although rather uncertain, the bolometric luminosity of LkH α 101 seems to be about a factor of 4 less than for S106IR, so it may be less massive or has evolved further onto the main sequence. A more evolved star may perhaps have evaporated more of its natal accretion disk or slowed its rotation rate, and hence the equatorial nature of the wind has become less pronounced.

The clumpy shell-like structure of the radio emission from LkH α 101 is reminiscent of some ultracompact H II regions such as W3(OH) (Dreher & Welch 1981). However, as for

S106IR the radio spectrum is very close to that expected for a stellar wind (Barsony et al. 1990) rather than the v^2 spectrum for uniform, optically thick, H II regions. As put forward for S1016IR (Drew et al. 1993) the strengths and ratios of the narrow H I line components (Simon & Cassar 1984) may indicate the existence of a dense ionized interaction zone between the stellar wind and ambient material which is so optically thick in the radio that the observed emission is dominated by the free-flowing stellar wind.

In summary, these first maps of the radio emission from luminous YSOs have provided valuable spatial information on

their winds. These data, when used together with the near-IR spectra, will enable progress to be made toward understanding the origin of the outflows in these young stars and thereby begin to fill in another missing piece in the high-mass star formation picture.

We thank the staff at NRAL for their assistance in making the observations with MERLIN and John Porter (Oxford) for communication of results on wind-disk interactions carried out as part of his thesis project. M. G. H. and J. E. D. acknowledge financial support of the SERC.

REFERENCES

- Bally, J., Snell, R. L., & Predmore, R. 1983, *ApJ*, 272, 154
 Barsony, M., Scoville, N. Z., Schombert, J. M., & Claussen, M. J. 1990, *ApJ*, 362, 674
 Becker, R. H., & White, R. L. 1988, *ApJ*, 324, 893
 Bjorkman, J. E., & Cassinelli, J. P. 1993, *ApJ*, 409, 429
 Chandler, C. J., Carlstrom, J. E., Scoville, N. Z., Dent, W. R. F., & Geballe, T. R. 1993, *ApJ*, 412, L71
 Churchwell, E., Felli, M., Wood, D. O. S., & Massi, M. 1987, *ApJ*, 321, 516
 Clark, B. G. 1980, *A&A*, 89, 377
 Dreher, J. W., & Welch, W. J. 1981, *ApJ*, 245, 857
 Drew, J. E., Bunn, J. C., & Hoare, M. G. 1993, *MNRAS*, in press
 Felli, M., Simon, M., Fischer, J., & Hamann, F. 1985, *A&A*, 145, 305
 Felli, M., Staude, H. J., Reddmann, T., Massi, M., Eiroa, C., Hefele, H., Neckel, T., & Panagia, N. 1984, *A&A*, 135, 261
 Felli, M., Taylor, G. B., Catarzi, M., Churchwell, E., & Kurtz, S. 1993, *A&AS*, 101, 127
 Garay, G. 1987, *Rev. Mexicana Astron. Af.*, 14, 489
 Hamann, F., & Persson, S. E. 1989, *ApJS*, 71, 931
 Herbig, G. H. 1971, *ApJ*, 169, 537
 Höflich, P., & Wehrse, R. 1987, *A&A*, 185, 107
 Hollenbach, D., Johnstone, D., & Shu, F. 1993, in *Massive Stars: Their Lives in the Interstellar Medium*, ed. J. P. Cassinelli & E. B. Churchwell (ASP Conf. Series 35), 26
 Lada, C. J. 1985, *ARA&A*, 23, 267
 Menten, K. N., & Reid, M. J. 1990, *BAAS*, 22, 1269
 Mozurkewich, D., Schwartz, P. R., & Smith, H. A. 1986, *ApJ*, 311, 371
 Owocki, S. P., Cranmer, S. R., & Blondin, J. M. 1993, preprint
 Persson, S. E., Geballe, T. R., McGregor, P. J., Edwards, S., & Lonsdale, C. J. 1984, *ApJ*, 286, 289
 Persson, S. E., McGregor, P. J., & Campbell, B. 1988, *ApJ*, 326, 339
 Pudritz, R. E., & Norman, C. A. 1986, *ApJ*, 301, 571
 Schmid-Burgk, J. 1982, *A&A*, 108, 169
 Simon, M., & Cassar, L. 1984, *ApJ*, 283, 179
 Simon, M., Felli, M., Cassar, L., Fischer, J., & Massi, M. 1983, *ApJ*, 266, 623
 Simon, M., Righini-Cohen, G., Fischer, J., & Cassar, L. 1981, *ApJ*, 251, 552
 Solf, J., & Carsenty, U. 1982, *A&A*, 113, 142
 Staude, H. J., Lenzen, R., Dyck, H. M., & Schmidt, G. D. 1982, *ApJ*, 255, 95
 Wright, A. E., & Barlow, M. J. 1975, *MNRAS*, 170, 41